

Adaptive and Multiple Time-scale Eligibility Traces for Online Deep Reinforcement Learning

Taisuke Kobayashi*

Nara Institute of Science and Technology, Nara, Japan

Abstract

Deep reinforcement learning (DRL) is one of the promising approaches to make robots accomplish complicated tasks. In the robotic problems with time-varying environment, online DRL is required since the methods that directly reuse the stored experience data cannot follow the change of the environment. Eligibility traces method is well known as an online learning technique to improve sample efficiency in the traditional reinforcement learning with linear regressors, not DRL. The one reason why the eligibility traces are not integrated with DRL is because dependencies between parameters of deep neural networks would destroy the eligibility traces. To mitigate this problem, this study proposes a new eligibility traces method that makes it possible to be applied even into DRL. The eligibility traces in DRL accumulate gradients computed based on the past parameters, which are different from that computed based on the latest parameters. Hence, the proposed method considers the divergence between the past and latest parameters to adaptively decay the eligibility traces. Instead of that divergence directly, Bregman divergences between outputs computed by the past and latest parameters, which are computationally feasible, are exploited. In addition, inspired by the replacing eligibility traces, a generalized method with multiple time-scale traces are newly designed. In benchmark tasks on a dynamic robotic simulator, the proposed method outperformed the conventional methods in terms of the learning speed and the quality of the tasks by the learned policy. A real-robot demonstration verified the importance of online DRL and the adaptability of the proposed method to the time-varying environment.

Keywords:

Deep reinforcement learning, Online learning, Eligibility traces

1. Introduction

As robotics has remarkably been developed in decades, the difficulty of tasks that autonomous robots are demanded to resolve is becoming higher. In particular, the tasks with complicated and unknown models (such as human assistance [1] and cloth manipulation [2]) are expected targets, although they are difficult to be resolved only by classic control methods. Reinforcement learning (RL) [3] and its extension combined with deep neural networks (DNNs) [4] to approximate policy and value functions, named deep reinforcement learning (DRL) [5, 6], would be the promising methodology for them.

As an open problem in robotics with DRL, we have to consider its sample efficiency. In general, RL needs many explorations to find the best task performance from scratch, and in addition, learning of DNNs is slower than that of shallow neural networks due to high nonlinearity and large number of parameters. Such sample inefficiency is not a big problem in video games [5] and stationary tasks

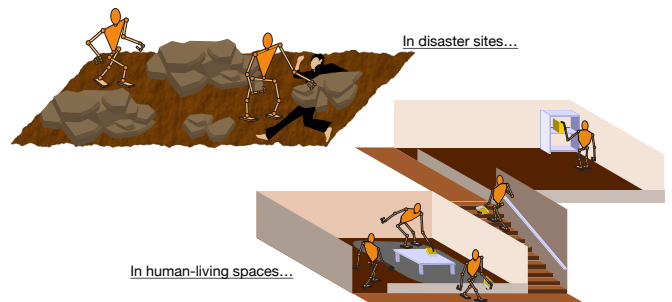


Figure 1: Open problem for autonomous robot learning: in real environments, the autonomous robots would face many different types of situations with corresponding tasks that are sometimes given on the spot, thereby making big data collection infeasible.

for industry that can collect big data in parallel [6], but it is infeasible for the autonomous robots. As illustrated in Fig. 1, real environments, such as disaster sites and human-living spaces, are non-stationary (or time-varying), and tasks in them are often given on the spot. Alternatively, the robots may change its kinodynamic characteristics by abrasion and/or deformation due to long-term operation. Such situations would prevent collecting sufficient data rapidly.

*Corresponding author

Email address: kobayashi@is.naist.jp (Taisuke Kobayashi)

URL: http://kbys_t.gitlab.io/en/ (Taisuke Kobayashi)

A naive but practical way to improve the sample efficiency is to store experiences and to replay them later, so-called experience replay [7]. This method can reuse the past experiences to update DNNs. However, in most cases where the autonomous robots have limited computational power and memory capacity, buffer size to store the experiences would be too much small to achieve the good performance [8]. In addition, as mentioned above, the autonomous robots sometimes should adapt to non-stationary tasks (e.g., adaptation to human preferences and/or system deterioration over time), and in that cases, the past experiences are no longer reusable.

On the other hand, by fully making use of the properties of RL (i.e., maximizing the sum of rewards in the future and Markovian), the prediction error at the current time is propagated to the past by combining the gradients on the past, so-called eligibility traces [3, 9, 10]. This propagation accelerates learning speed by reusing the past gradients. However, this method is well known as the method only for the traditional RL with linear regressors. It is reported that DRL with the eligibility traces method tends to fail learning [11], although shallow neural networks can relatively easily be integrated with it [12].

The reason why the eligibility traces fails is explained by Van et al. [10, 11] that the eligibility traces method is backward-view approximation of λ -return [3, 13], which leaves approximation errors. Although only for linear regressors, such errors have been eliminated by the literature [10]. If only that, however, the reason why the standard eligibility traces can utilize with linear regressors is not explained clearly.

As another reason, it is found that the difference between the linear and nonlinear regressors is in parameter-dependent gradients. All the gradients stored in the eligibility traces are implicitly assumed to be gained from the same parameters. This assumption is satisfied if the gradients are independent from parameters like the linear regressors. In the nonlinear regressors like DNNs, however, the gradients are depending on the other parameters, in particular the parameters of the front layers in DNNs. That is, the divergence between the gradients computed by the parameters before and after updates (let us call the *gradient divergence*) would be caused as the failure reason. Although the shallow networks (e.g., only one hidden layer) makes the gradient divergence ignorable due to minimal parameter dependency [12], the deep networks have to face it.

Hence, this paper focuses on how to mitigate the effects of the dependency on the parameters in DNNs. To this end, an adaptive eligibility traces method, which aims to decay the eligibility traces adaptively according to the gradient divergence, is proposed as a first contribution. Although such decaying is a conservative way, the proposed method can work when recent parameters are updated only slightly. The practical problem is however raised that the gradient divergence is difficult to be computed analytically or efficiently. In practice, therefore, this paper uti-

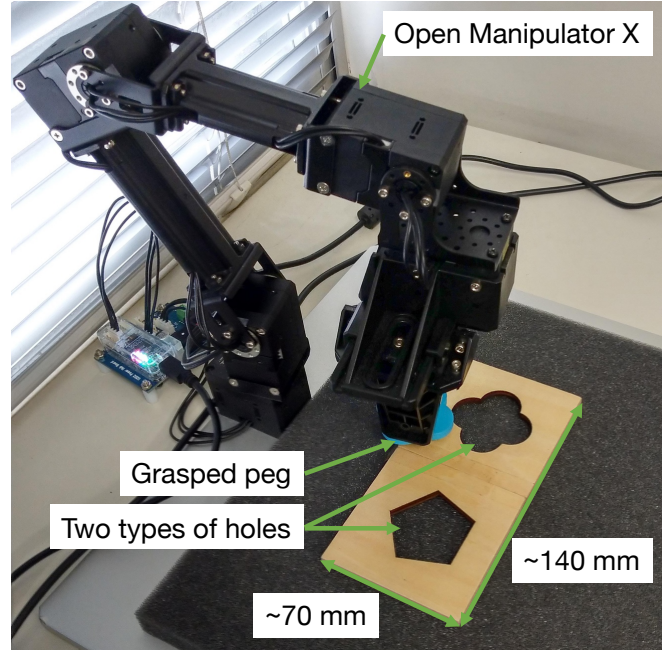


Figure 2: Peg-in-hole task by a four-axis robot arm with a one-axis gripper: the task is initialized with holding the peg that fits either of the holes on the left or right, and the robot aims to insert the peg into the hole; after learning with one peg, it is exchanged with another to demonstrate adaptability to changes in the problem.

lizes the Bregman divergences [14] between the past and latest outputs, which imply the gradient divergence and are computed analytically with low computational cost.

Furthermore, we focus on the fact that the replacing eligibility traces method [9] resets the traces if the latest gradient becomes dominant. This resetting behavior would mitigate the accumulation of the gradient divergence. Inspired by this resetting behavior, a generalized eligibility traces method with multiple time-scale traces is further proposed. This proposed method includes the standard and replacing eligibility traces according to the setting of the decaying factors. It is expected that, with the appropriate parameters, the proposed method can achieve the benefits of both the standard and replacing eligibility traces.

For verification of the two proposed methods, four robotic benchmark tasks, which include the tasks that either of the standard or replacing eligibility traces methods is poor at, are conducted in a dynamic simulator. Although the contribution of the adaptive decaying to the learning performance is not so pronounced, the generalized eligibility traces show the excellent performance in all the tasks and exceed the conventional methods.

Finally, a time-varying peg-in-hole task is demonstrated using a robot arm, Open Manipulator X developed by Robotis (see Fig. 2). Even when the target pair of peg and hole is exchanged after learning for another pair and the past experience data would be no longer reused, the proposed method for online DRL enables the robot to acquire its new target.

2. Preliminaries

2.1. Reinforcement learning

2.1.1. Problem statement

RL makes an agent learn the optimal policy, which can achieve the maximum return (i.e., the sum of rewards) from an environment [3]. Here, Markov decision process (MDP) is assumed as the tuple $(\mathcal{S}, \mathcal{A}, \mathcal{R}, p_0, p_T, \gamma)$. First, the agent gets the initial state $s_0 \in \mathcal{S}$ randomly: $s_0 \sim p_0(s_0)$. At the time step $t \in \mathbb{N}$, the agent samples an action $a_t \in \mathcal{A}$ from the policy π over the current state $s_t \in \mathcal{S}$: $a_t \sim \pi(a_t | s_t)$. The sampled action a_t acts on the environment, and the next state s_{t+1} is sampled according to the transition probability model p_T : $s_{t+1} \sim p_T(s_{t+1} | s_t, a_t)$. In addition, the agent gets a reward $r_t \in \mathcal{R}$ according to the reward function: $r_t = r(s_t, a_t, s_{t+1})$. In this interaction loop, the agent aims to maximize the return defined as $R_t = \sum_{k=0}^{\infty} \gamma^k r_{t+k}$ where $\gamma \in [0, 1)$ by optimizing the policy to π^* . Note that, only if the transition probability model p_T and the reward function r are stationary, the past raw experiences can be reused to enhance the sample efficiency [7].

In many methods, the expected value of the return, named the value function, is approximated as $V(s_t) = \mathbb{E}[R_t | s_t]$. If we have the correct V , π^* only needs to choose the action that can maximize V . To learn V , a temporal difference (TD) error δ_t , which should be minimized, is derived from Bellman equation.

$$\delta_t = r_t + \gamma V(s_{t+1}) - V(s_t) \quad (1)$$

Note that, to learn the action value function Q , We can replace $V(s)$ to $Q(s, a)$.

2.1.2. Actor-critic algorithm

Actually, the policy π and the value function V are black-box functions, hence it is difficult to learn them directly. Regression methods are therefore needed to approximate such functions through optimization of their parameters θ . Note that approximation by DNNs are introduced later.

To learn the optimal parameters, loss functions to be minimized should be designed. In this paper, two loss functions for an actor (with the policy), \mathcal{L}_a , and a critic (with the value function), \mathcal{L}_c , are minimized according to actor-critic algorithms [15, 16, 17, 18]. When the policy and value functions are approximated with the parameters θ_n after n updates, $\pi(a | s; \theta_n)$ and $V(s; \theta_n)$, they are defined as follows:

$$\mathcal{L}_a(t, \theta_n) = -\hat{\delta}_t \log \pi(a_t | s_t; \theta_n) \quad (2)$$

$$\mathcal{L}_c(t, \theta_n) = -\hat{\delta}_t V(s_t; \theta_n) \quad (3)$$

where $\hat{\cdot}$ cuts the computational graph and changes the variable to just value. $\mathcal{L}_a(t, \theta_n)$ is derived from the policy gradient method [19], and $\mathcal{L}_c(t, \theta_n)$ is equivalent to the minimization of the squared TD error.

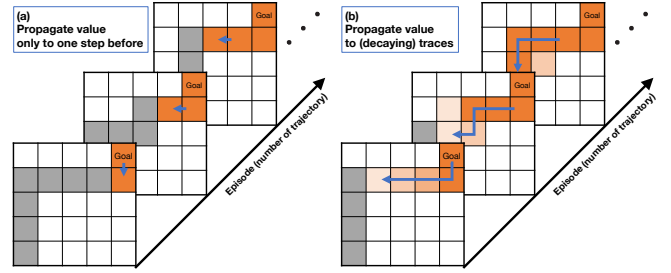


Figure 3: Advantage of eligibility traces: in the left (a), many visits are required to back propagate future information to the initial state; in the right (b), using the eligibility traces, future information can be back propagated effectively.

In addition, the importance sampling [20] is applied. Although the importance sampling technique is for off-policy learning, it can be applied to online on-policy learning without storing the past parameters as follows. Suppose that the agent interacts with the environment before updating the policy, and to update the policy in parallel during the interaction. In that case, the action a_t for the interaction has to be sampled from the policy with θ_{n-1} , while a_t is used for updating the policy with θ_n .

$$\rho_{t,n} = \frac{\pi(a_t | s_t; \theta_n)}{\pi(a_t | s_t; \theta_{n-1})} \quad (4)$$

By combining these equations, the main loss function is derived.

$$\mathcal{L}(t, \theta_n) = \hat{\rho}_{t,n} \{ \mathcal{L}_a(t, \theta_n) + \mathcal{L}_c(t, \theta_n) \} \quad (5)$$

Finally, this loss function is minimized basically using stochastic gradient decent (SGD) methods like Adam [21]. Note that the latest regularization techniques [15, 16, 17] can be integrated in this basic algorithm.

2.2. Eligibility traces

The parameters are updated to minimize the above loss function \mathcal{L} at each time step, but in that case, the propagation of the future rewards to the vicinity of the initial state is too slow, as shown in the left of Fig. 3. To accelerate such propagation, the eligibility traces [3, 9, 10], e , utilize the trajectory given by MDP, as shown in the right of Fig. 3.

That is, the past gradients are accumulated and used to update the parameters as follows:

$$g_t = \frac{\nabla_{\theta_n} \mathcal{L}(t, \theta_n)}{\hat{\delta}_t} \quad (6)$$

$$e_t = \gamma \lambda e_{t-1} + g_t \quad (7)$$

$$\theta_{n+1} = \theta_n - \alpha \text{SGD}(\hat{\delta}_t e_t) \quad (8)$$

where $\alpha \in \mathbb{R}_+$ denotes the learning rate and $\text{SGD}(\cdot)$ is one of the SGD methods. $\lambda \in [0, 1]$ means the rate of decaying. The eligibility traces are initialized as zero when starting a new trajectory (i.e., at $t = 0$). Note that, since all the

components in \mathcal{L} as shown in eqs. (2) and (3) are multiplied by δ_t , this accumulation can be computed stably.

If $\lambda = 0$, this method is consistent with the TD learning without the eligibility traces. If $\lambda = 1$ and the tasks to be resolved have time limitation, this method represents Monte Carlo method. With large λ , the propagation would be facilitated, thereby improving the sample efficiency.

As a variant of the standard eligibility traces, the replacing eligibility traces [9] have been proposed for the table-style value function. The original replacing eligibility traces can be extended for the general approximation of the policy and value functions as follows:

$$e_t = \begin{cases} g_t & |g_t| > |e_{t-1}| \\ \gamma \lambda e_{t-1} & \text{otherwise} \end{cases} \quad (9)$$

That is, this method stores only the most dominant gradients into e . Although such a replacing operation does not satisfy the backward-view approximation of λ -return, the better learning performance than by the standard eligibility traces has been reported.

2.3. Deep neural networks

When DNNs are employed for approximation of the policy and the value function, θ is basically given to be weights w and biases b for the respective hidden layers and an output layer. That is, the outputs from the respective hidden layers x_i ($i = 1, \dots, L$) with L number of layers are defined as follows:

$$x_i = f_i(w_i^\top x_{i-1} + b_i) \quad (10)$$

where x_0 is set as the inputs (s in DRL). The activation functions, $f_i(\cdot)$, are given for nonlinearity, and they are usually common for all the layers, $f_i(\cdot) = f(\cdot)$.

Finally, the outputs from the last hidden layer is mapped to the domain for the learning targets y .

$$y = m(w_o^\top x_L + b_o) \quad (11)$$

where $m(\cdot)$ denotes the mapping function, such as a soft-plus function for positive real domain, a sigmoid function for $[0, 1]$, and so on.

3. Adaptive eligibility traces

3.1. Problem and solution

Let us theoretically derive the problem hidden in the eligibility traces with the nonlinear regressor (see Fig. 4). Then, a basic idea of its solution is proposed (details are introduced from the next section).

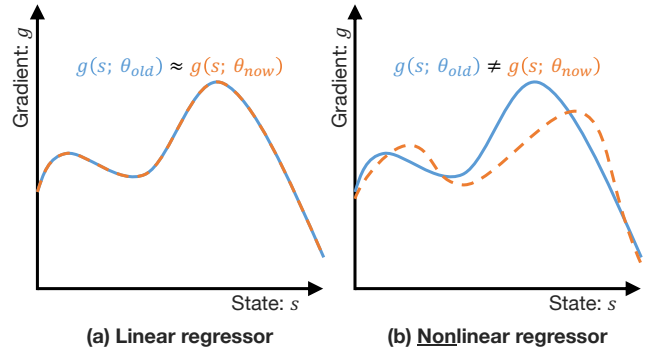


Figure 4: Parameter dependency of gradient in nonlinear regressor: unlike the linear regressor shown in the left (a), the nonlinear regressor has the different gradients between the past and latest parameters, as shown in the right (b).

3.1.1. Case of linear regressor

The eligibility traces method accumulates the gradients w.r.t the parameters, and uses them again and again until they are completely decayed. If the linear regressors, e.g., $\theta = w$ and $y = m(w^\top x(s))$ with $x(\cdot)$ the fixed function that maps to higher dimensions, the gradients of y w.r.t w are given as follows:

$$\nabla_{\theta_n} y = m'(w_n^\top x(s)) x(s) \quad (12)$$

where $m'(\cdot)$ denotes the derivative of the mapping function $m(\cdot)$. In addition, the gradients after updating the parameters by $\Delta\theta_n = \theta_{n+1} - \theta_n \ll 1$ is derived as follows:

$$\nabla_{\theta_{n+1}} y = m'(w_n^\top x(s) + \Delta w_n^\top x(s)) x(s) \quad (13)$$

If the outputs are real by $m(x) = x$ (and $m'(x) = 1$), the above equation is no longer depending on the parameters. Even if the outputs are in limited spaces like the positive real one, the effects of parameter update is easy to be ignored since $m'(\cdot)$ can be smooth and smaller than 1, such properties of which can derive $m'(x + \Delta x) - m'(x) < \Delta x$.

3.1.2. Case of nonlinear regressor

In contrast, however, the nonlinear regressors like DNNs cannot ignore the effects of parameter update in the gradients. Specifically, $x(s)$ in eq. (12) is replaced with x_i ($i = 1, \dots, L$), which is depending on the parameters on $j < i$ layers: $x_i(s; \theta_{j < i})$. In addition, y is computed multiplication of the features depending on $\theta_{\neq o}$, $x_L(s; \theta_{\neq o})$, and θ_o . Such highly parameter-dependent gradients may not be reusable for updating the latest parameters as the eligibility traces since they are absolutely different from the gradients computed by the latest parameters and violate SGD. Here, the difference between the gradients computed by the past and latest parameters are defined as the *gradient divergence*, $\Delta g(t, \theta_n) = g(t, \theta_{n+1}) - g(t, \theta_n)$.

3.1.3. Solution

Theoretically, the gradient divergence is one possibility why the eligibility traces in DNNs fail, as mentioned

Algorithm 1 Proposed algorithm

```
1:  $n \leftarrow 0$ 
2: Initialize  $\theta_0$ 
3: while True do
4:    $t \leftarrow 0$ ,  $e = 0$ , and assume  $\theta_{n-1} = \theta_n$   $\triangleright$  Reset
5:    $s_0 \sim p_0(s_0)$ 
6:   while True do
7:     Compute  $\pi(s_t; \theta_n), V(s_t; \theta_n)$ 
8:      $a_t \sim \pi(a_t | s_t; \theta_n)$ 
9:     Execute  $a_t$ 
10:    if  $t \neq 0$  then  $\triangleright$  During interaction if possible
11:      Compute the gradient  $g_t$ 
12:      using eqs. (1)–(6)
13:      Compute the adaptive decaying factor  $\lambda_{t,n}^d$ 
14:      using eqs (14)–(17)
15:      Update parameters to  $\theta_{n+1}$ 
16:      using eqs. (19) and (20)
17:      Compute  $\pi(s_t; \theta_{n+1}), V(s_t; \theta_{n+1})$ 
18:       $n \leftarrow n + 1$ 
19:    end if
20:     $s_{t+1} \sim p_T(s_{t+1} | s_t, a_t)$ 
21:     $t \leftarrow t + 1$ 
22:    if Meet end conditions then
23:      break
24:    end if
25:  end while
26: end while
```

in the above. To eliminate this, the naive solution is to recompute the loss functions given by the past states, actions, and rewards (i.e., to directly use λ -return [3, 11, 13]), although that requires high computational cost and memory capacity. The advantages of the eligibility traces are in low computational cost and memory efficiency, which are suitable for online learning in the autonomous robots. Hence, we have to modify the eligibility traces somehow by mitigating or avoiding the adverse effects of the gradient divergence.

As a solution, this paper proposes the way to adaptively decay the eligibility traces with the large gradient divergence, although that would be conservative. To do so, the gradient divergence should be defined quantitatively. The next section, therefore, introduces the definition of the output divergences as alternative to the gradient divergence. According to the output divergences, the adaptive decaying method is proposed.

In addition, the resetting behavior of the replacing eligibility traces method [9] would implicitly mitigate the accumulation of the gradient divergence. Inspired by this fact, a generalized eligibility traces method with multiple time-scale traces, which contains the standard and replacing eligibility traces methods, is further proposed.

In summary, the implemented algorithm is written in Alg. 1.

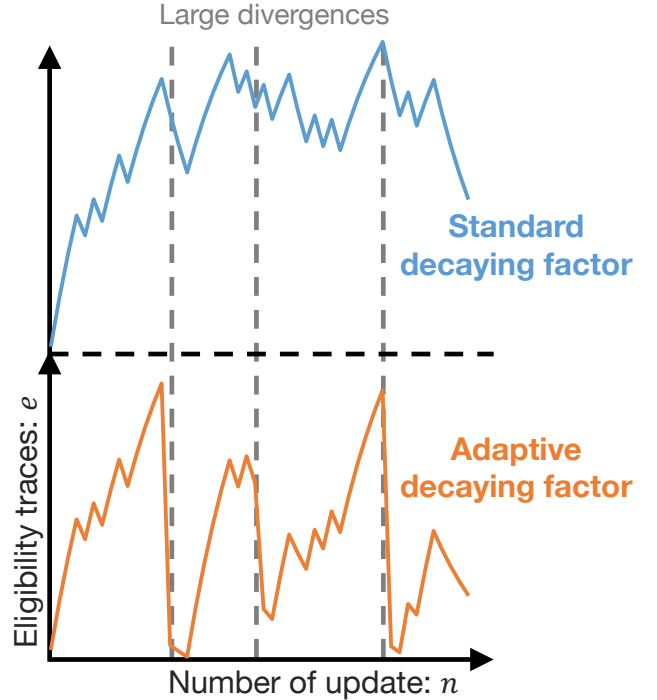


Figure 5: Behavior of the adaptive decaying factor: if the large divergences happen, the adaptive decaying resets the eligibility traces since the stored gradients no longer indicate the correct update direction.

3.2. Output divergences as alternative to gradient divergence

As mentioned in the above, the gradient divergence is difficult to be defined in computationally cheap way due to huge parameter space. Instead, we focus on that the outputs of regressors, i.e., the policy π and the value function V , are in relatively small spaces and reveal the change in the parameters. That is, the gradient divergence is approximated as the combination of two output divergences of π and V .

By considering the types of the respective spaces, the divergences are generally given as Bregman divergence [14]. Specifically, the divergence of π , which is in probability space, is given as Kullback-Leibler (KL) divergence.

$$\begin{aligned} d_{t,n}^\pi &= \text{KL}(\pi(a | s_t; \theta_n) | \pi(a | s_t; \theta_{n-1})) \\ &= \int_a \pi(a | s_t; \theta_n) \log \rho_{t,n}(a) da \end{aligned} \quad (14)$$

Note that, in most cases, this integral can be solved with a closed-form solution for the model that is employed for the policy (e.g., normal distribution). In addition, the divergence of V , which is in Euclid space, is given as L2 norm.

$$d_{t,n}^V = \frac{1}{2} \{V(s_t; \theta_n) - V(s_t; \theta_{n-1})\}^2 \quad (15)$$

As a remark, even in the cases without the closed-form solution of KL divergence, Pearson divergence [22] would alternate with it.

$$d_{t,n}^\pi = \int_a \pi(a | s_t; \theta_{n-1}) (\rho_{t,n}(a) - 1)^2 da$$

Since this definition is based on a squared loss, the Pearson divergence always satisfies positive even if the Monte Carlo approximation is performed, although the KL divergence does not.

Using the above two divergences, d^π and d^V , λ for adaptively decaying the eligibility traces are defined as follows:

$$d_{t,n}^s = \lambda_{t,n-1}^d d_{t,n-1}^s + (d_{t,n}^\pi + d_{t,n}^V) \quad (16)$$

$$\lambda_{t,n}^d = \exp(-\kappa d_{t,n}^s) \quad (17)$$

$$\lambda_{t,n} = \lambda_{\max} \lambda_{t,n}^d \quad (18)$$

where λ_{\max} is the maximum of the decaying factor since $d^\pi, d^V > 0$, and $\lambda = \lambda_{\max}$ in the standard method. κ denotes the gain to adjust the ease of decaying.

d^s accumulates the divergences while decaying adaptively. If d^π and d^V are instantaneously large (i.e., the parameters are largely changed), the eligibility traces e defined in eq. (7) are reset since the accumulated gradients are likely to be different from that computed by the latest parameters. If $(1 - \lambda^d)d^s \simeq d^\pi + d^V$, the decaying speed and the accumulated divergences are balanced, and λ^d would converge on the specific value (less than 1). That means, the decaying factor is adjusted stationally. Otherwise, the gradients would be accumulated to e like the standard method does (see Fig. 5).

3.3. Generalization to include replacing eligibility traces

As shown in eq. (9), the replacing eligibility traces discard all the past gradients if the new gradient exceeds the stored one. This discarding is expected to work similar to the above adaptive decaying. However, on the other hand, the replacing eligibility traces would run short of propagation of the latest value to the past by cutting the trajectory. Hence, to exploit the benefits of the replacing eligibility traces while accumulating the trajectory information, a generalized eligibility traces are proposed in this section.

Let us define e^i ($i = 1, \dots, K$) with $K > 1$ as multiple time-scale traces. They are with a K -series-layered structure, and the maximum decaying factor of i -th layer, λ_{\max}^i , is given. Under these conditions, a new update rule to replace conventional ones (i.e., eqs (7) and (8) for the standard version and; eqs (9) and (8) for the replacing version) is proposed as follows:

$$e_t^i = \begin{cases} e_t^{i-1} & i \neq 1 \wedge \Delta e_t^{i-1} > 0 \\ \gamma \lambda_{\max}^i \lambda_{t,n}^d e_{t-1}^{i-1} + \beta^i g_t & \text{otherwise} \end{cases} \quad (19)$$

$$\theta_{n+1} = \theta_n - \alpha \text{SGD}(\hat{\delta}_t e_t^K) \quad (20)$$

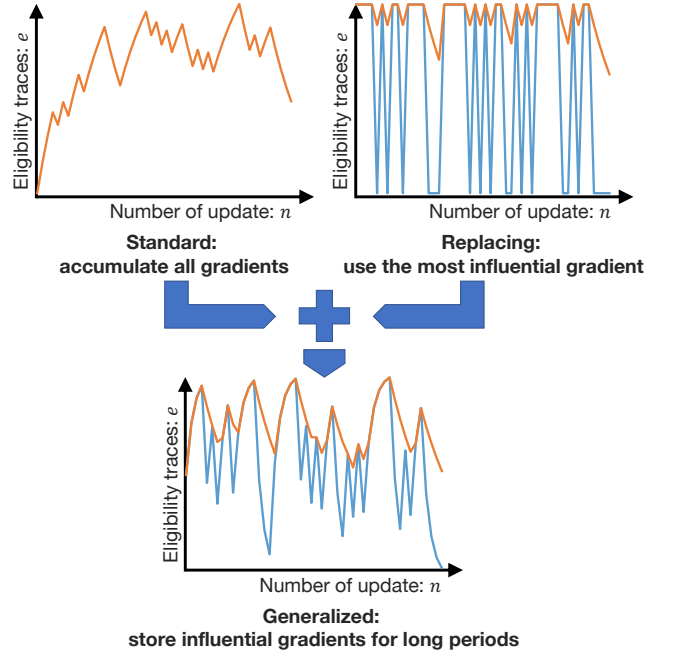


Figure 6: Behavior of the generalized eligibility traces: by having two different time-scale traces, this new method can accumulate the gradients as like the standard eligibility traces, and store them for long periods by replacing them into another traces as like the replacing eligibility traces.

where $\Delta e_t^i = e_t^{i-1} - e_{t-1}^{i-1}$. β^i is the sequence with three conditions: $\beta^i \geq \beta^{i+1}$, $\sum_{i=1}^K \beta^i = 1$, and $\beta^K = 0$. For example, the following arithmetic sequence satisfies the above conditions:

$$\beta^i = \frac{2(K-i)}{K(K-i)} \quad (21)$$

This update rule implies that the gradient propagates from shallow to deep layers, which have the different time constants for decaying. Note that the condition for replacing is relaxed to make the sign reversal between layers true. Such relaxation would allow the update direction to rapidly follow the latest gradient direction.

The large K wastes memory capacity of systems and loses the advantages of the eligibility traces in comparison with the experience replay. Therefore, K is fixed on two in this paper, which is the minimum value to gain the benefits from the replacing eligibility traces. In fact, although the above equations are given as a general form, it can easily be imagined that the effects of deepening the layer is not so critical due to the effects of the adaptive decaying, which resets all the traces adaptively.

In the case with $K = 2$, the proposed eligibility traces can generalize the standard/replacing eligibility traces. Specifically, we expect three modes according to the setting of λ_{\max}^1 and λ_{\max}^2 as follows (also, see Fig. 6):

1. $\lambda_{\max}^1 > \lambda_{\max}^2$: The second layer decays its traces faster than the first layer, that is, we can expect $e_t^1 \simeq$

e_t^2 . Specifically, if all the gradients are positive (or negative) or $\lambda_{\max}^2 = 0$, this mode perfectly matches the standard eligibility traces.

2. $\lambda_{\max}^1 = 0$ and $\lambda_{\max}^2 > 0$: Since $e_t^1 = g_t$, this mode is almost the same as the replacing eligibility traces. The difference is only whether the sign reversal is included in the replacing condition.
3. $0 < \lambda_{\max}^1 < \lambda_{\max}^2$: The traces with the short-term memory e^1 replace the traces with the long-term memory e^2 only if e^1 may be more influential than e^2 . As a result, only the most important traces are actively stored for long periods. Such a behavior can be regarded to be similar to hyperbolic discounting, which has been studied as biologically-plausible decision making mechanism with variable decaying speeds [23, 24].

From the above analysis, the third mode should be better than the others. To exploit the advantages of both the standard and replacing eligibility traces, it is expected that $\lambda_{\max}^2 \simeq 2\lambda_{\max}^1$ would be reasonable choice.

4. Simulations

4.1. Benchmark tasks

In the dynamic simulations, the agent learns the given tasks, which have $|\mathcal{S}|$ -dimensional state space and $|\mathcal{A}|$ -dimensional action space, through E episodes with up to $T = 1000$ time steps. After learning, the agent performs the learned task 50 times to compute the sum of rewards for each, and median of them is given to be the score. The agent with different random seeds tries to learn each task 20 trials for statistical evaluation.

Four benchmark tasks for DRL simulated by Pybullet Gym [25, 26] are prepared. They are listed in Table 1 (also see Fig. 7). Their purposes (i.e., their reward designs) are given as follows:

- (a) InvertedPendulum: A cart keeps a pole standing.
- (b) Swingup: A cart swings up a pole and keeps it standing.
- (c) HalfCheetah: A two-dimensional cheetah with two legs walks forward as fast as possible.
- (d) Ant: A three-dimensional quadruped walks forward as fast as possible.

4.2. Conditions

Basic network architecture, which is implemented by PyTorch [27], is shown in Fig. 8. The tasks conducted are without image input state. Therefore, only L fully connected layers with N neurons are employed. To avoid over fitting, layer normalization [28] is added after each layer except the output one. As an activation function, Swish function [29, 12] is employed for biological plausibility and high nonlinearity.

Using this network architecture, the actor and critic approximate the policy π and value function V , respectively. Specifically, as the policy model, student-t distribution [18], which has location parameter $\mu \in \mathbb{R}^{|\mathcal{A}|}$, scale parameter $\sigma \in \mathbb{R}_+^{|\mathcal{A}|}$, and degrees of freedom $\nu \in \mathbb{R}_{\geq 2}$ as parameters to be approximated, is employed. Since σ and ν are in positive real domain, softplus function is used as the mapping function. The others (i.e., μ and V) are in real domain, so identity map is used.

To stably learn the tasks, the latest policy regularization techniques are combined. Specifically, the importance sampling is replaced by PPO [15] with a clipping value ϵ . The policy entropy regularization based on SAC [16] is added with a regularization weight β_{DE} . The TD regularization [17] is also introduced with a regularization weight β_{TD} . In addition, for robustness to noisy gradients in online learning, a robust SGD, i.e., LaProp [30] with t-momentum [31] and d-AmsGrad [32] (so-called td-AmsProp), is employed with their default parameters except the learning rate.

Table 2 summarizes the common hyperparameters to be used in the simulations. Here, these parameters were tuned empirically using CartPoleContinuousBulletEnv-v0. In addition, the hyperparameters related to the proposed method, $(\lambda_{\max}^1, \lambda_{\max}^2, \kappa)$, are set as the following comparative conditions.

1. (0.0, 0.0, 0.0) as no eligibility traces
2. (0.9, 0.0, 0.0) as the standard eligibility traces
3. (0.0, 0.9, 0.0) as the replacing eligibility traces
4. (0.9, 0.0, 1.0) as the adaptive standard eligibility traces
5. (0.0, 0.9, 1.0) as the adaptive replacing eligibility traces
6. (0.5, 0.9, 1.0) as the proposed eligibility traces

Here, $\lambda_{\max} = 0.9$ is given based on the preferred value for the standard eligibility traces. Through tuning, it is empirically found that the better κ is within [1.0, 10.0].

The importance of the eligibility traces will be confirmed by comparing the first condition with the others. The adaptive decaying will be verified by comparing the standard/replacing eligibility traces with/without it. The proposed eligibility traces with multiple time-scale traces will also be verified by comparing the last three conditions.

4.3. Results

First, to confirm the learning tendency, the test results with the respective scores (i.e., the sum of rewards at each episode) are summarized in Fig. 9. Overall, the DRL without the eligibility traces failed to learn all the tasks. In contrast, the eligibility traces accelerated learning and enabled the agent to acquire the given tasks. The proposed decaying technique in eqs. (14)–(17) did not improve the performance of the tasks significantly, although the medians indicated as the lines in the boxes were likely to be increased by the adaptive decaying with $\kappa = 1$. The reason

Table 1: Simulation environments provided by Pybullet Gym [25, 26]

ID	Name	State space $ \mathcal{S} $	Action space $ \mathcal{A} $	Episode E
InvertedPendulumBulletEnv-v0	InvertedPendulum	5	1	200
InvertedPendulumSwingupBulletEnv-v0	Swingup	5	1	200
HalfCheetahBulletEnv-v0	HalfCheetah	26	6	2000
AntBulletEnv-v0	Ant	28	8	2000

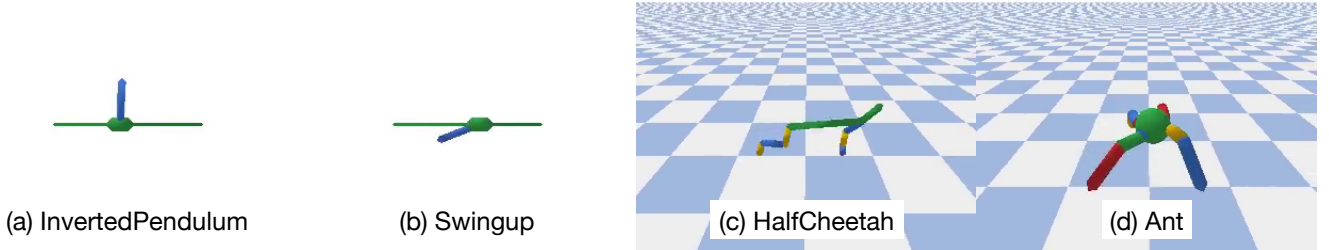


Figure 7: Snapshots of four benchmark tasks: they are simulated by Pybullet Gym [25, 26]; (a) InvertedPendulum makes a cart keep a pole standing; (b) Swingup makes a cart swing up a pole on it standing; (c) HalfCheetah makes a two-legged robot walk forward as fast as possible. (d) Ant makes a four-legged robot walk forward as fast as possible.

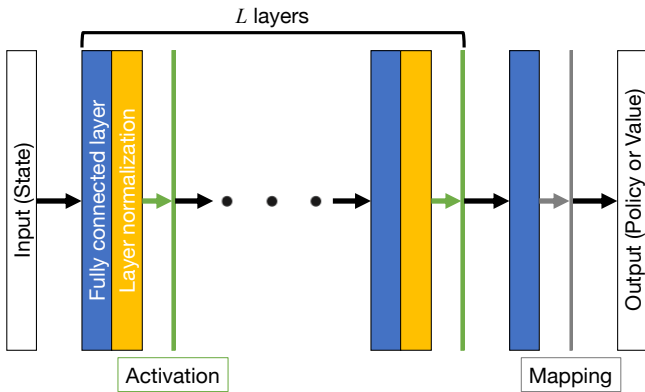


Figure 8: Network architecture in actor for policy or critic for value function: the input is given to L modules, which are connected in series; each module is composed of a fully connected layer, a layer normalization, and an activation function; an additional fully connected layer uses for shaping the features given by L modules to the output.

why the standard eligibility traces without the adaptive decaying succeeded in learning more than expected would be that the latest regularization techniques [15, 16, 17] suppress the amount of parameter update, and secondarily reduce the gradient divergence, which is considered as the reason why the eligibility traces are unsuitable for DRL.

Remarkably, the proposed integration technique in eqs. (19) and (20) outperformed the others in all the tasks. Whereas the standard/replacing eligibility traces have the task-specific performances especially in the locomotion tasks (HalfCheetah and Ant tasks), mostly because of the integrated characteristics, the proposed eligibility traces exhibited the high performance in both tasks. Hence, we can agree that the both proposed techniques for the eligibility traces (in particular, the generalized ver-

Table 2: Common hyperparameters for the simulations

Symbol	Meaning	Value
N	Number of neurons	128
L	Number of layers	5
γ	Discount factor	0.99
α	Learning rate	1e-4
ϵ	Threshold for clipping	0.1
β_{DE}	Gain for entropy regularization	0.025
β_{TD}	Gain for TD regularization	0.025

sion with multiple time-scale traces) improved the learning performance efficiently.

The learning behaviors of the score are shown in Fig. 10. In addition, the average of the adaptive decaying factors λ^d in each episode is depicted in Fig. 11. We found that the decaying tends to be strengthened when the score changes greatly (in particular, increases). This is a natural behavior since the policy and value functions would be greatly updated when the performance is improved. In fact, in the proposed method with the highest performance (0.5, 0.9, 1.0), the decaying was stronger overall than that in the others. By focusing on the learning curves in Fig. 10, we also found that the proposed method basically increased the scores from the beginning of learning. That is, we can say that the proposed method enhanced the sample efficiency without reusing the past experiences directly.

5. Demonstration with real robot experiments

5.1. Peg-in-hole task

As a real-robot-used demonstration of the proposed method, a peg-in-hole task with a robot arm is performed

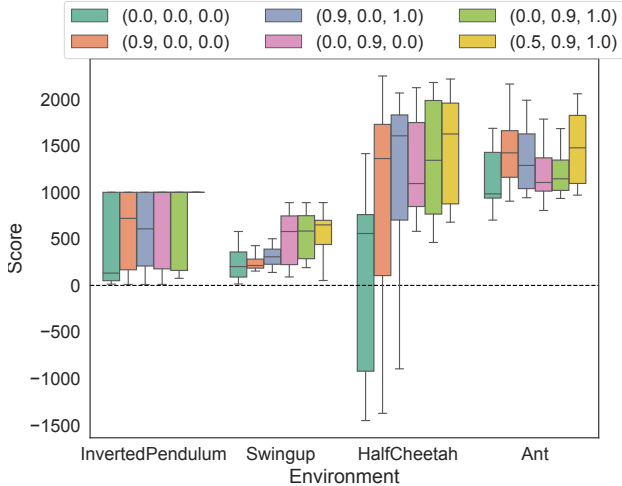


Figure 9: Test results of four benchmark tasks illustrated as box plots: the tuples on legend denote $(\lambda_{\max}^1, \lambda_{\max}^2, \kappa)$; although the contribution of the adaptive decaying was not significant, we found improvements at the median level; thanks to the integration of the standard and replacing eligibility traces, the proposed method (with yellow) outperformed the others in all the tasks.

(see Fig. 2). The robot used is Open Manipulator X developed by Robotis, which has one axis for yaw rotation; three axes for pitch rotation; and one axis for a gripper. That is, the robot can control the position of its end effector while keeping the gripper vertical. However, it should be noted that the position control is not sufficiently accurate and the control error may occur.

Two types of pegs with different shapes are prepared, and either of them are grasped by the robot from the beginning of episode. Two 70 mm squared plates, each of which has the hole corresponding to either of pegs in the center, are set side by side on the environment. The depth of each hole is around 5 mm. Note that cushions are attached on the bottom of the plates and pegs to reduce the load when insertion is attempted deviated from the center of holes. In this setting, the working space of the end effector is within $[p, \bar{p}]$ (see Table 3).

As state space for RL, the three-dimensional observed and commanded positions of the end effector are employed. To utilize the load as collision detection, the observed currents on four axes (without the actuator for the gripper) are added (roughly within [-500 mA, 500 mA] for each current). From the control error and the load, the flag of collision ($\in [0, 1]$) is stochastically given. In total, the 11-dimensional state space is constructed.

The action space is given to be three-dimensional: the velocity of the end effector in Cartesian space, which is integrated into the commanded position by Euler method. The velocity of the end effector is bounded within 0.01, 0.015, and 0.005 m/s for x -, y -, z -axes, respectively. In addition, the commanded position is also clipped within $[p, \bar{p}]$. In the control loop of the robot (with around 3 Hz), as the probability of the collision is increased, a proportional feedback control is activated so that the commanded

position returns to the collision point (i.e., the current observed position).

To design a reward function, we define the purpose of this task as reaching the target position in the corresponding hole while reducing load as much as possible. This purpose is implemented as the following reward function:

$$r = \exp(-k\|p^{\text{obs}} - p^{\text{tar}}\|_{\Sigma}^2) - f_c + \begin{cases} \pm 100 & p_z^{\text{obs}} \leq p_z^{\text{tar}} \\ 0 & \text{otherwise} \end{cases} \quad (22)$$

where p^{obs} denotes the observed position of the end effector, p^{tar} is the target position (i.e., the rough position of the center of the hole). Σ is for scaling the axes by the ranges of the commanded position $[p, \bar{p}]$, and k denotes the gain for sparsity. f_c denotes the stochastic flag of collision. If the peg is inserted into the correct hole, the successful bonus 100 is given; and if the peg is inserted into the wrong hole, the big penalty -100 is given. Whether the inserted hole is correct or not is roughly judged according to $(p_y^{\text{obs}} p_y^{\text{tar}}) > 0$. In both cases, that episode is terminated and a new episode is started after initialization. Note that the first term for approaching the target is auxiliary because the accurate target position cannot be specified in the environment that is not precisely built while only the last sparse term would make the task intractable.

To demonstrate the effectiveness and adaptability of the eligibility traces, the following demonstration is performed. Here, it is noticed that the proposed eligibility traces with $(\lambda_{\max}^1, \lambda_{\max}^2, \kappa) = (0.5, 0.9, 1.0)$ outperformed the conventional ones in the above simulations, only the proposed method represents the eligibility traces. At the first stage, the robot tries to insert the peg with flower shape into the hole on the left side, and the method with/without the eligibility traces are compared to show the sample efficiency of the eligibility traces even in real robot experiment. After the first stage, the peg is exchanged with the one with pentagon shape for the hole on the right side, and the robot continues to learn the peg-in-hole task with the different target as the second stage. Since the robot can only perceive this change from the reward signals, the past raw experiences at the first stage would prevent the robot from adapting to the new target. Even in that case, the eligibility traces would adapt the robot to the change of the target efficiently due to no reuse of the past raw experiences.

The above configurations are summarized in Table 3. To accomplish this task, the proposed method with the same parameters as Table 2 except for the learning rate is employed. Since the real robot experiment would contain large uncertainty due to observation and control noises, the learning rate α is reduced to 5×10^{-5} for stable learning. The length of episodes in each stage is differently given: 200 episodes for the first stage and; 100 episodes for the second stage.

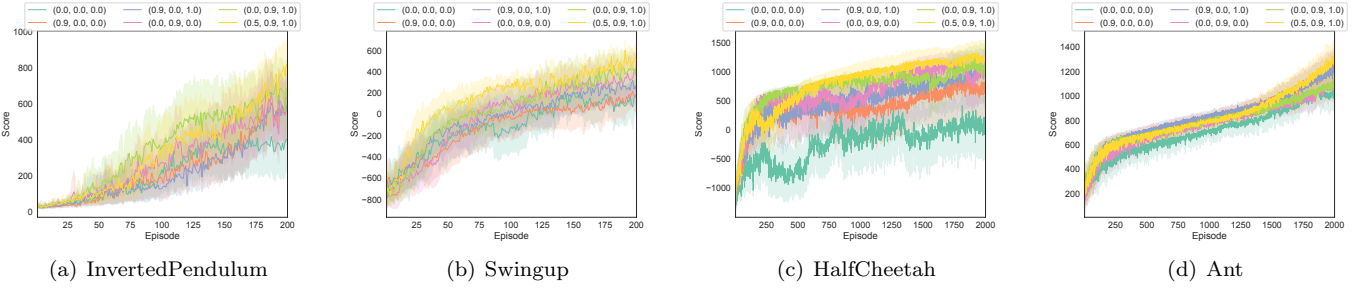


Figure 10: Learning curves of four benchmark tasks: the sum of rewards at each episode are given as the score; the corresponding shaded areas show the 95 % confidence intervals; the proposed method (with yellow) increased the return rapidly, and outperformed the others in total.

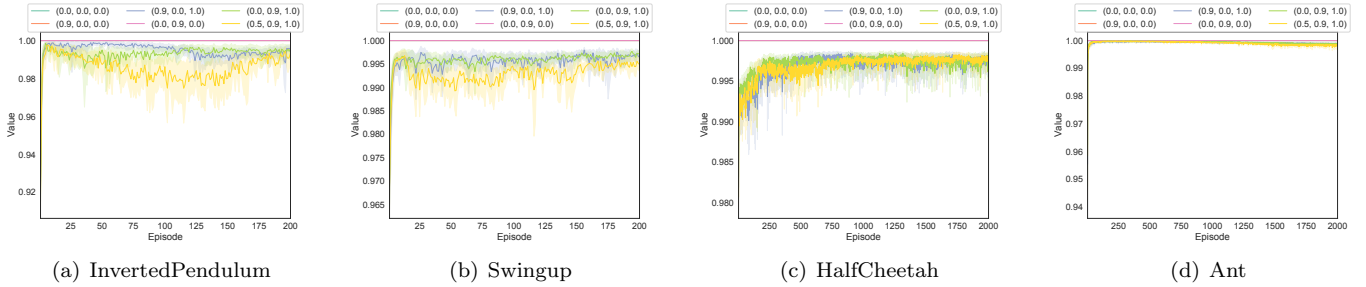


Figure 11: Average λ^d of four benchmark tasks: the corresponding shaded areas show the 95 % confidence intervals; the proposed method (with yellow) decayed the eligibility traces more frequently than the cases with (0.9, 0.0, 1.0) and (0.0, 0.9, 1.0); the frequent decaying implies that the parameters θ were actively updated and the optimization progressed appropriately.

5.2. Results

The learning curves from three trials are depicted in Fig. 12. The successful snapshots of the test results at the times pointed in Fig. 12 (i.e., the ends of the respective stages) are also shown in Fig. 13.

During the first stage, the robot had the peg corresponding to the hole with flower shape on the left side of the robot. As can be seen in Fig. 12, the case without the proposed eligibility traces was mostly trapped into local optima, and could not insert the peg into the corresponding hole. In contrast, the proposed eligibility traces accelerated learning speed and yielded the peg insertion many times during learning. After finishing the first stage (at 200 episode), the robot succeeded in demonstrating the acquired peg-in-hole skill as shown in Fig. 13(a) (also see the attached video).

After the first stage, the peg grasped by the robot was exchanged with the one corresponding to the hole with pentagon shape on the right side of the robot. Since the robot did not know this fact, at the beginning of the second stage, the robot failed to approach the correct hole, and got large penalty by inserting the peg grasped into the wrong hole. However, after these failures, the robot started to look for the new target, and found it on the opposite side. Thanks to the knowledge how to insert the peg into the hole (i.e., the pushing down motion has large reward), the robot could rapidly adapt to the new target by fully utilizing the streaming data without storing the

past experiences.

5.3. Discussion

Consequently, we illustrated the effectiveness of the eligibility traces method, and its improvement by the proposed adaptive and multiple time-scale eligibility traces. Compared to the simulation results, however, the learning curves of the real robot experiments are not stable yet, suggesting the need to develop new learning methods and regularization techniques that are robust to the noise occurred in the real environment. In particular, when using the eligibility traces, robustness is extremely important because stable learning gradients derived from the average of a large amount of data cannot be utilized. However, we have to take care with appropriate adjustment of the trade-off between conservative learning and sample efficiency so as not to cause a reduction in sample efficiency for the sake of conservative learning.

6. Conclusion

This paper proposed the new eligibility traces with the adaptive decaying and the multiple time-scale traces for sample-efficient DRL without storing raw experiences. The gradient divergence was considered as the reason why the DRL with the eligibility traces tends to fail learning. Therefore, when the output divergence (instead of the gradient divergence in pursue of low computational cost) is

Table 3: Configurations for peg-in-hole task

Symbol	Meaning	Value
$ \mathcal{S} $	State space	11
$ \mathcal{A} $	Action space	3
T	Maximum time step	180 (~ 60 s)
E	Number of episodes	(200, 100)
\underline{p}	Lower bound of position	(0.09 m, -0.07 m, 0.024 m)
\overline{p}	Upper bound of position	(0.16 m, 0.07 m, 0.044 m)
p^{ini}	Initial position	(0.1 m, 0.0 m, 0.04 m)
p^{tar}	Goal position	(0.125 m, ± 0.035 m, 0.025 m)
k	Gain for reward scaling	5.0

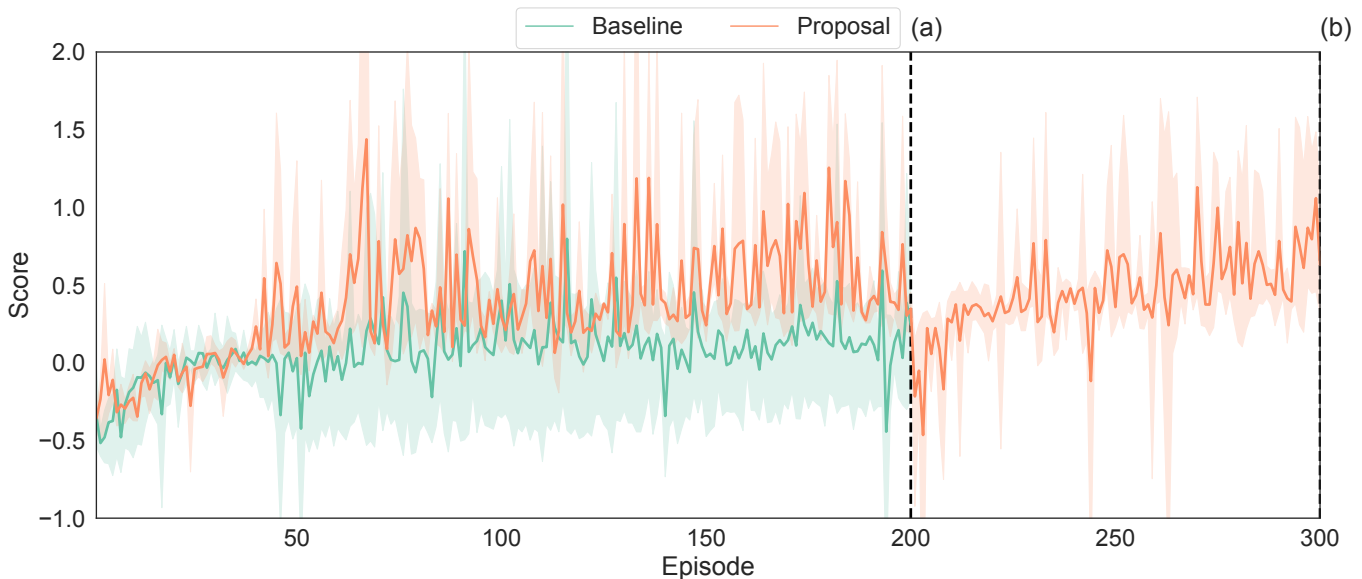


Figure 12: Learning curves by DRLs without/with the proposed eligibility traces (Baseline and Proposal, respectively): score in the vertical axis denotes the mean of the rewards obtained in each episode; after 200 episodes, the peg grasped was exchanged for the new target; the proposal accelerated learning speed and yielded the peg insertion, while the baseline hardly achieved the task; even after exchanging the peg grasped and the target, the proposal properly adapted the robot to that difference by fully utilizing the streaming data.

increased, the accumulated traces are reseted by adjusting the decaying factor adaptively. In addition, the replacing operation in the replacing eligibility traces would mitigate the adverse effects of the gradient divergence. To introduce this capability, the new update rule with the generalized eligibility traces, which include the standard and replacing ones, was designed for mitigating the adverse effects while keeping the ability to accumulate the gradients for the sample efficiency.

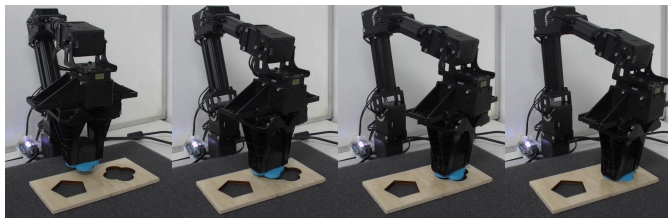
To verify the proposed method, four types of simulations were first conducted. The generalized eligibility traces outperformed in comparison with the conventional versions in terms of the sum of rewards obtained by the trained policies and the sample efficiency. In particular, while the strengths of the standard and replacing eligibility traces varied, the proposed method enabled the agent to solve all the tasks stably by inheriting their characteristics. The peg-in-hole demonstration using a robot arm was also performed. We confirmed that, even if the tar-

get (i.e., the reward function) was changed with time, the robot could achieved the new target by efficiently following the target change.

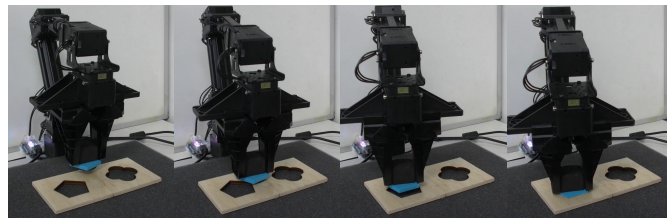
Future work is to theoretically investigate the optimal design of the generalized eligibility traces. In addition, to accelerate learning furthermore, model-based RL [33, 34] is one of the promising approaches, hence, the proposed method will be integrated with it while carefully considering catastrophic forgetting of the model learned [35]. After establishing the sample-efficient online DRL, we will apply it to more complicated real-world applications with autonomous robots.

Acknowledgements

This work was supported by JSPS KAKENHI, Grant-in-Aid for Scientific Research (B), Grant Number 20H04265.



(a) At the end of the first stage



(b) At the end of the second stage

Figure 13: Snapshots at the times pointed in Fig. 12: in both stages, the robot succeeded in inserting the peg into the corresponding hole.

References

- [1] H. Modares, I. Ranatunga, F. L. Lewis, D. O. Popa, Optimized assistive human–robot interaction using reinforcement learning, *IEEE transactions on cybernetics* 46 (3) (2015) 655–667.
- [2] Y. Tsurumine, Y. Cui, E. Uchibe, T. Matsubara, Deep reinforcement learning with smooth policy update: Application to robotic cloth manipulation, *Robotics and Autonomous Systems* 112 (2019) 72–83.
- [3] R. S. Sutton, A. G. Barto, *Reinforcement learning: An introduction*, MIT press, 2018.
- [4] A. Krizhevsky, I. Sutskever, G. E. Hinton, Imagenet classification with deep convolutional neural networks, in: *Advances in neural information processing systems*, 2012, pp. 1097–1105.
- [5] D. Silver, A. Huang, C. J. Maddison, A. Guez, L. Sifre, G. Van Den Driessche, J. Schrittwieser, I. Antonoglou, V. Panneershelvam, M. Lanctot, et al., Mastering the game of go with deep neural networks and tree search, *nature* 529 (7587) (2016) 484.
- [6] S. Levine, P. Pastor, A. Krizhevsky, J. Ibarz, D. Quillen, Learning hand-eye coordination for robotic grasping with deep learning and large-scale data collection, *The International Journal of Robotics Research* 37 (4-5) (2018) 421–436.
- [7] L.-J. Lin, Self-improving reactive agents based on reinforcement learning, planning and teaching, *Machine learning* 8 (3-4) (1992) 293–321.
- [8] T. L. Hayes, N. D. Cahill, C. Kanan, Memory efficient experience replay for streaming learning, in: *International Conference on Robotics and Automation, IEEE*, 2019, pp. 9769–9776.
- [9] S. P. Singh, R. S. Sutton, Reinforcement learning with replacing eligibility traces, *Machine learning* 22 (1-3) (1996) 123–158.
- [10] H. Van Seijen, A. R. Mahmood, P. M. Pilarski, M. C. Machado, R. S. Sutton, True online temporal-difference learning, *The Journal of Machine Learning Research* 17 (1) (2016) 5057–5096.
- [11] H. van Seijen, Effective multi-step temporal-difference learning for non-linear function approximation, *arXiv preprint arXiv:1608.05151* (2016).
- [12] S. Elfving, E. Uchibe, K. Doya, Sigmoid-weighted linear units for neural network function approximation in reinforcement learning, *Neural Networks* 107 (2018) 3–11.
- [13] J. Schulman, P. Moritz, S. Levine, M. Jordan, P. Abbeel, High-dimensional continuous control using generalized advantage estimation, in: *International Conference on Learning Representations*, 2016.
- [14] L. M. Bregman, The relaxation method of finding the common point of convex sets and its application to the solution of problems in convex programming, *USSR computational mathematics and mathematical physics* 7 (3) (1967) 200–217.
- [15] J. Schulman, F. Wolski, P. Dhariwal, A. Radford, O. Klimov, Proximal policy optimization algorithms, *arXiv preprint arXiv:1707.06347* (2017).
- [16] T. Haarnoja, A. Zhou, P. Abbeel, S. Levine, Soft actor-critic: Off-policy maximum entropy deep reinforcement learning with a stochastic actor, *arXiv preprint arXiv:1801.01290* (2018).
- [17] S. Parisi, V. Tangkaratt, J. Peters, M. E. Khan, Td-regularized actor-critic methods, *Machine Learning* (2019) 1–35.
- [18] T. Kobayashi, Student-t policy in reinforcement learning to acquire global optimum of robot control, *Applied Intelligence* (2019) 1–13.
- [19] R. J. Williams, Simple statistical gradient-following algorithms for connectionist reinforcement learning, *Machine learning* 8 (3-4) (1992) 229–256.
- [20] S. T. Tokdar, R. E. Kass, Importance sampling: a review, *Wiley Interdisciplinary Reviews: Computational Statistics* 2 (1) (2010) 54–60.
- [21] D. P. Kingma, J. Ba, Adam: A method for stochastic optimization, *arXiv preprint arXiv:1412.6980* (2014).
- [22] K. Pearson, X. on the criterion that a given system of deviations from the probable in the case of a correlated system of variables is such that it can be reasonably supposed to have arisen from random sampling, *The London, Edinburgh, and Dublin Philosophical Magazine and Journal of Science* 50 (302) (1900) 157–175.
- [23] H. Rachlin, L. Green, Commitment, choice and self-control 1, *Journal of the experimental analysis of behavior* 17 (1) (1972) 15–22.
- [24] S. Kobayashi, W. Schultz, Influence of reward delays on responses of dopamine neurons, *Journal of neuroscience* 28 (31) (2008) 7837–7846.
- [25] G. Brockman, V. Cheung, L. Pettersson, J. Schneider, J. Schulman, J. Tang, W. Zaremba, Openai gym, *arXiv preprint arXiv:1606.01540* (2016).
- [26] E. Coumans, Y. Bai, Pybullet, a python module for physics simulation for games, robotics and machine learning, *GitHub repository* (2016).
- [27] A. Paszke, S. Gross, S. Chintala, G. Chanan, E. Yang, Z. DeVito, Z. Lin, A. Desmaison, L. Antiga, A. Lerer, Automatic differentiation in pytorch, in: *Advances in Neural Information Processing Systems Workshop*, 2017.
- [28] J. L. Ba, J. R. Kiros, G. E. Hinton, Layer normalization, *arXiv preprint arXiv:1607.06450* (2016).
- [29] P. Ramachandran, B. Zoph, Q. V. Le, Swish: a self-gated activation function, *arXiv preprint arXiv:1710.05941* 7 (2017).
- [30] L. Ziyin, Z. T. Wang, M. Ueda, Laprop: a better way to combine momentum with adaptive gradient, *arXiv preprint arXiv:2002.04839* (2020).
- [31] W. E. L. Ilboudo, T. Kobayashi, K. Sugimoto, Tadam: A robust stochastic gradient optimizer, *arXiv preprint arXiv:2003.00179* (2020).
- [32] T. Kobayashi, Towards deep robot learning with optimizer applicable to non-stationary problems, *arXiv preprint arXiv:2007.15890* (2020).
- [33] T. G. Thrunthel, E. Falotico, F. Renda, C. Laschi, Model-based reinforcement learning for closed-loop dynamic control of soft robotic manipulators, *IEEE Transactions on Robotics* 35 (1) (2018) 124–134.
- [34] I. Clavera, V. Fu, P. Abbeel, Model-augmented actor-critic: Backpropagating through paths, *arXiv preprint arXiv:2005.08068* (2020).
- [35] T. Kobayashi, T. Sugino, Reinforcement learning for quadrupedal locomotion with design of continual–hierarchical curriculum, *Engineering Applications of Artificial Intelligence* 95 (2020) 103869.